A Theoretical Basis for the Reflected of Acoustic Chirp Signals from Aircraft Wake Vortices With Measured Examples.

A.L. Martin, Wake Watch Pty Ltd.

andrew.martin@wakewatch.com.au

Introduction.

This paper sets out to achieve four things, these are;

1. Refractive index reflected from wake vortices;
2. Measurements of vortex core diameters for two different aircraft;
3. Measurements of wake vortex characteristics;
4. The effects of atmospheric inversions on vortex lifetime;
5. Conclusions.

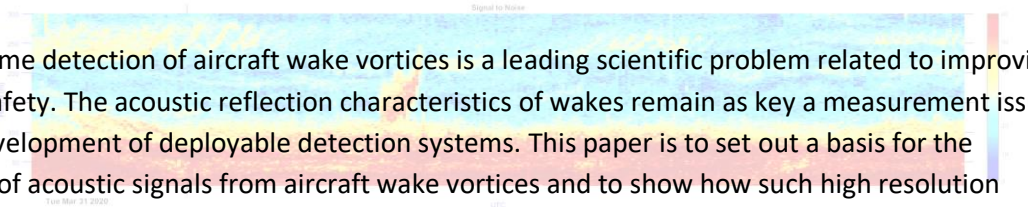

The real-time detection of aircraft wake vortices is a leading scientific problem related to improving aviation safety. The acoustic reflection characteristics of wakes remain as key a measurement issue for the development of deployable detection systems. This paper is to set out a basis for the reflection of acoustic signals from aircraft wake vortices and to show how such high resolution reflected signals can be integrated to obtain the velocity flow field within an wake vortex. This provides the first ever real time, very high resolution measurements of the vortex velocity field. The very high resolution measurements provided by a chirp SODAR can provide resolution of 0.2m over a range of 90m with measurements every 1.57 seconds or 0.7 m resolution to a range of 320m with measurements every 2.93 seconds and provides unprecedented views of the wake velocity field and the interaction of the wake with the atmosphere. A description of the SODAR vortex reflected signals are outlined from basic theory. By using the velocity fluctuation, a simple expression can be derived for obtaining the tangential velocity profiles from chirp SODAR measurements. Some example SODAR velocity profiles are derived from measurements and serve to provide new insights about the structure and the demise processes in aircraft wake vortices. This also provides key information about the role of inversion layers in prolonging the life of wake vortices, particularly as the long lived wake vortices evolve in a different way to those used for modelling. This suggests that the current models may be inappropriate to develop any understanding of wake vortex behaviour in very low turbulence atmospheres.

These new findings about the wake vortex structure could fill the vortex knowledge gaps about the nature of long lasting vortices for departure and arrival, particularly when inversion layers are present and help understand high-altitude vortex behaviour[1].

1. Refractive index reflections from wake vortices

The reflected wake vortex signals detected by the chirp SODAR are generated by two different mechanisms which are described by Burnham[2] below.

The most relevant observation is that "If the pressure drop in the vortex core is great enough, it can generate a coherent, direct reflected signal. If the vortex core is perpendicular to the acoustic beam, this signal can be much larger than turbulence scattering because the scattered signal spreads out in a plane, not all space. Core scattering is Doppler shifted by the vertical motion of the core as a whole, not the flow field in the core"[2]. This indicates that for core scattering the velocity field of the core does not produce any Doppler shift, the only Doppler shift is due to the fall of the vortex. This provides a path to understanding how the vortex reflected signal can be used to obtain the vortex velocity field.

The scattering of sound occurs at small-scale in-homogeneities of the field of acoustic refractive index. Bradley[3] states that " For a fluctuation $\underline{V'}$ in the vector wind, the sound speed fluctuation depends on the direction of $\underline{V'}$ compared to the direction of propagation $\underline{\hat{k}}$ of the sound ($\underline{\hat{k}}$ is a unit vector). The combination of temperature and velocity fluctuations gives refractive index fluctuations

$$n' = \frac{\underline{V\prime} \cdot \underline{\hat{k}}}{c} + \frac{T\prime}{2T} \qquad (1)$$

where *c* in the speed of sound and *T* is the temperature and *T'* is the temperature fluctuation.

The following chiefly relates to SODARs since they obtain a signal through reflections from turbulence. The SODAR beam and pulse duration τ define a volume that contains refractive index fluctuations n' continuously varying in strength and spatial scale.

This is very instructive as equation 1 indicates that velocity fluctuations such as occur within a vortex produce refractive index changes that are capable of producing very strong reflected acoustic signals[1], signals that are directly related to the velocity fluctuations $\underline{V'}$.

Obtaining the vortex velocity flow field.

A viscous vortex consists of a swirling flow field with approximately circular streamlines. In the Rankine vortex model [4] , tangential velocity $\underline{V_r}$ along flow streamlines increases linearly with radius *r*, and decreases inversely with radius *r* outside the core.

A generalised description of a vortex vector wind can then be given as being proportional to the inverse of the vortex radius such that

$$\underline{V_r} \propto 1/r \qquad (2)$$

where $\underline{V_r}$ is the vector wind at the radius r within the vortex.

By differentiation, the velocity fluctuation as a function of the radius is then

$$\underline{V_r}' \propto {}^{1}/_{r^2} \qquad (3)$$

Each point in the velocity field has an associated vector wind or tangential velocity which by differentiation along the vortex radius yields the velocity fluctuation. The whole vortex space may be thought of as being threaded by vortex velocity lines which are everywhere tangent to the local velocity and is shown in Figure 1.

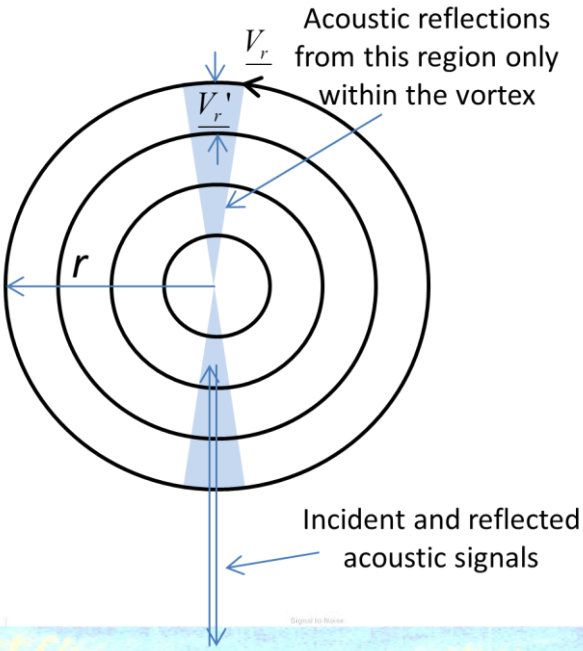

Figure 1. Simplified vortex structure where the velocity is given by equation 2. The velocity increases as the inverse of the radius so that the maximum velocity is in the core at small radii. The vortex core is located in the centre of the vortex at r = 0. The dominant acoustic reflections are assumed to be only from regions where the vortex velocity is substantially perpendicular to the incident acoustic signals. This means that close to the core the reflection is from a very small area while further towards the outside of the vortex the reflection area is larger, this is called the radar cross section (RCS) which varies a 1/r.

The tangential velocity field Vr of the vortex at radius r shown in Figure 1 can be represented by the Rankine model[10] .

$$Vr = \begin{cases} \Gamma r/(2\pi R^2) & r \leq R \\ \Gamma/(2\pi r) & r \geq R \end{cases} \quad (4)$$

where Γ is the circulation, and R is the core radius.

Using a circulation of 160m^2/s with a core radius of 1m is shown in Figure 2. The Rankine model is compared to a measured wake vortex from a B738 at 4 seconds after the aircraft is overhead showing that the model fits the measurement very well and validates the use of a Rankine model. The wake measurement is the of the application of equation (7) to the measurement data.

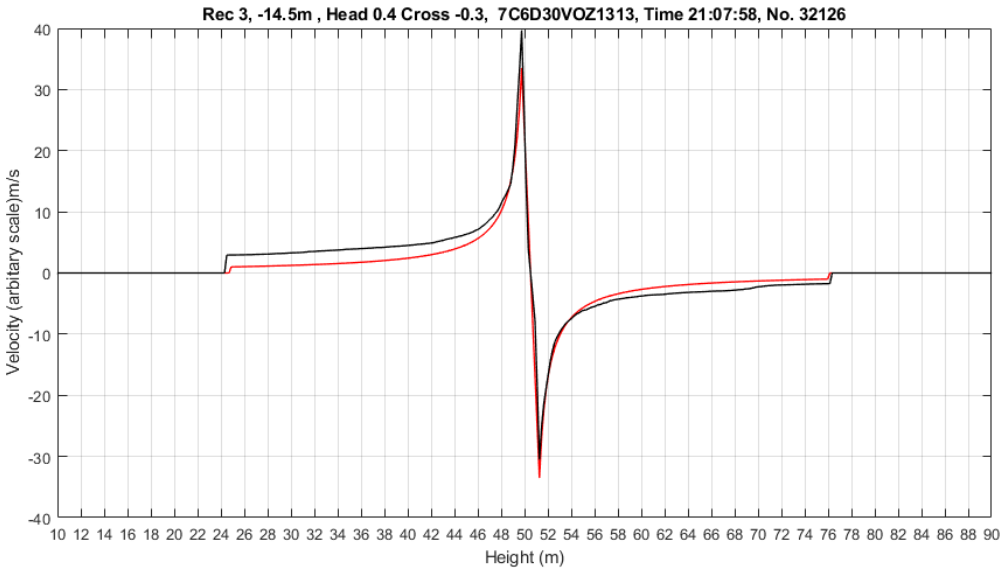

Figure 2. Rankine wake vortex model for a B738 with a core radius of 1m and a circulation of 160m^2/s. This is compared to a measured wake vortex of a B738 at 4 seconds after the aircraft was overhead of the wake array. Complete measurement of this arrival is shown in Figure 6.

Equations 1 and 3 can now be combined for the vortex to give the refractive index as a function of radius so that (We can ignore the temperature contribution as it is much smaller)

$$n_r{}' = \frac{\underline{V'_r} \cdot \underline{\hat{k}}}{c} \qquad (4)$$

This indicates that as the velocity fluctuations are radial, then the refractive index variation is also radial and the acoustic signals can only be reflected from the refractive index changes along a radius. This also indicates that there will be no Doppler shift of the signals reflected from along a radius as the velocity of the vortex is perpendicular to the radius.

From[3], the amplitude (of the SODAR signal) from a single velocity fluctuation is proportional to $n_r{}'$.

This then indicates that the amplitude of the return SODAR signals S_a at any point along a radius is linear function proportional to the velocity fluctuations at that point

$$S_a \propto \underline{V'_r} \qquad (5)$$

or the change in vortex velocity as a function of radius. This result from the amplitude of the backscattered signal level is a magnitude only does not yield any velocity sign.

As the reflected signal level S_a varies as $1/r_c$, Fig. 1, this effect of the RCS must be compensated for by an additional multiplication of the reflected signal S_a so that the estimation of the vortex velocity structure is consistent across the whole vortex.

Thus

$$S_a / r_c \quad \propto \underline{V'_r} \qquad (6)$$

Thus by integrating the signal level obtained from the velocity fluctuations we can obtain the vortex velocity field as a function of the vortex radius

$$\underline{V_r} \propto \int_{-r}^{r} \underline{V'_r \, dr} \qquad (7)$$

This provides a very simple linear method for obtaining wake vortex velocity field by adding up the return signal levels to obtain the shape of the vortex velocity. It does not give any direct means of obtaining the exact velocity as that will only come by calibrating the system by the use of an external reference such as previous measurements of aircraft wake vortices, such previous measurements are point measurements at a 15m radius and are not continuous velocity field measurements and there may be some difficulty in making exact comparisons.

In 2005 it was stated that[6] "Due to the major difficulties connected with measurements in the vicinity of high-Reynolds-number wake vortex cores, there is no common agreement on the actually prevailing tangential velocity profiles in wake vortices". The development of this new technique for estimating actual wake vortex velocity profiles will lead to a greatly improved understanding of wake vortex evolution and their interaction with the atmosphere.

The next issue is the method by which the integration in (7) can be carried out using the backscattered signal level data. By assuming that the velocity of the vortex at it outer edges is zero so that

$$Vr(\Gamma > 0,\ r \gg R) = 0 \qquad (8)$$

and that at the centre of the vortex the velocity is zero so that

$$Vr(\Gamma > 0,\ r = 0) = 0 \qquad (9)$$

The critical measurements required for performing the integration of (7) are the position of the core and the position of the vortex core maximum velocities, these measurements allow the integration of (7) to proceed in four stages. These positions can be obtained using the backscatter signal level from (5) and the assumptions of equations (8 and 9). The core position is found by integrating the entire signal level (5) and assumes that the sum of the velocity fluctuations within the vortex is the same for the upper and lower halves of the vortex so that

$$\sum_{-r}^{0} Vr = \sum_{0}^{r} Vr \qquad (10)$$

and assumes that the vortex is symmetrical in the vertical plane as shown in Figure 1.

To locate the vortex centre the signal levels are first all added up for all the data points *n* to give the total of the backscattered signal levels TSa.

$$TSa = \sum_{1}^{n} Sa \qquad (11)$$

The core of the vortex is then located at the data point *nc* where

$$TSa/2 = \sum_{1}^{nc} Sa \qquad (12)$$

This yields the vortex core position as well as the upper and lower vortex outer edges. The next step after locating the core position is to apply the radar cross section scaling (6), to correct the measured signal to account for the change in RCS with change in the vortex radius, see Figure 1.
To apply the RCS correction the location of the core is required.

After the location of the core is determined and the RCS correction applied, the position of the maximum core velocities can now be obtained using the assumption of equations (8 and 9) using the same process as used to find the core position except that now the core position (where the velocity of the vortex is zero) is used as the starting point. This yields the upper and lower vortex core edges.

This yields 5 points by which the 4 integrations to obtain the vortex velocity profile can proceed in the direction indicated, the integrations for (7) are then:

1/ upper outer vortex edge to the upper core edge,
2/ core position to upper core edge,
3/ core position to lower core edge,
4/ lower outer vortex edge to lower core edge.

The next issue is that the resulting vortex produced by integration needs to be scaled to obtain the correct velocity profile. Obtaining the scale factor is the result of accurately assessing many components associated with the use of the SODAR technique together with an assessment of the acoustic reflectivity of the vortex structure.

The acoustic RADAR equation is given in Ref. 11, equation 4.26. This equation has some variables for which it is difficult to arrive at exact values. The equation also contains loss components due to propagation which are distance and humidity dependent.

The distant dependent part is also complex and difficult to evaluate exactly as the vortex target is a tubular structure and is not a point target. This indicates that the radar cross section component in one dimensional and that the resulting loss is linear with distance and not the distance squared loss. There is also a humidity dependent loss which is in dB/meter. As these two propagation loss components are distance dependent they need to be compensated for before any other calculations set out above are applied.

After the distance dependent losses are corrected, the rest of the processes can be applied as above, but the other independent system losses set out in the RADAR equation need to be compensated for, the best way to do this is to use a scaling factor which is derived from calibration of the system against other known wake vortex circulations for any given aircraft.

2. Measurements of vortex core diameters for two different aircraft

Some example measurements using the signal level integration technique are given in the next section to provide the first ever direct measurements of the vortex velocity field in high resolution. Figure 3 shows the wake array used to make the wake turbulence measurements. The associated wind profiler are the black baffles to the left while the wake array is to the right starting from the yellow baffles.

Figure 3. Wake array at Melbourne Airport showing bi-static acoustic transceivers of the 8 used to make wake vortex measurements. The array is set across the 16 approach at 990m from the 16 threshold. The positions of each of the transceivers relative to the centre line is shown in the titles to the 8 transceiver measurements in Figures 5, 11 and 14.

There is probably also a thermal contribution to the refractive index through small scale temperature variations through the dissipation rates of TKE by viscosity and of thermal variance by conduction within the wake. When pressure decreases, so does the temperature, when pressure increases, so does the temperature. A vortex is a low pressure event introduced to a given air mass by the passing of the aircraft so the inner vortex temperature goes down[2]. This temperature effect will allow low level signals to be reflected from other parts of the vortex so that Doppler shift measurements can be made. The very high level signals from the velocity fluctuations dominate the weaker signals from the temperature fluctuations which makes using the Doppler to measure vortex velocity very difficult.

Wake Vortex Structure

Figure 4 shows the calculated turbulence around a wake vortex[5]. The vortex core is evident as a confined circular structure and the turbulence around the core which is associated with the vortex interaction with the atmosphere is also evident. The example measurements that follow show the agreement of theory and measurements.

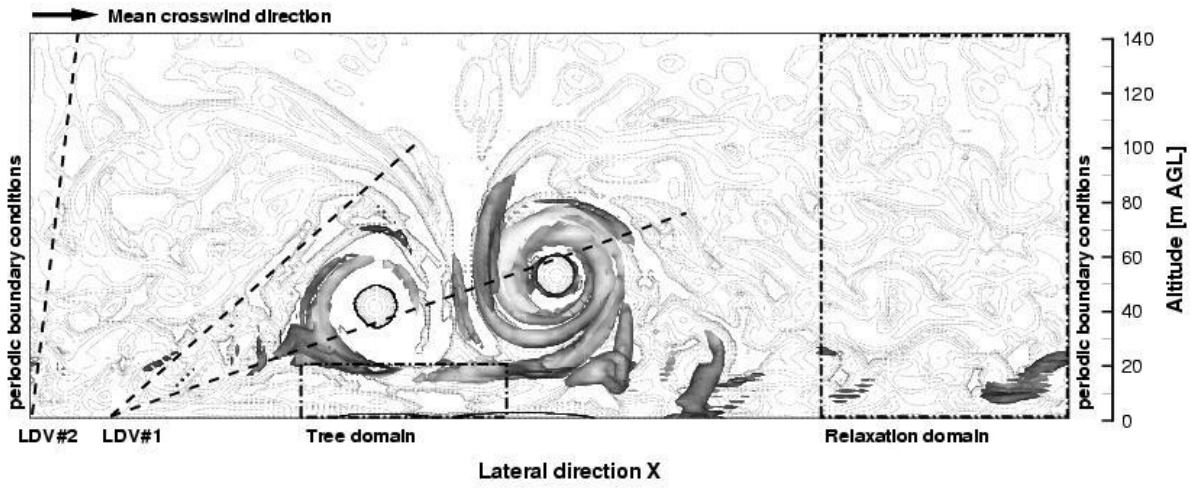

Figure 4. Calculated turbulence around wake vortices. The main vortex cores are well defined with circular turbulent flow patterns while the vortex turbulent interaction with the atmosphere is also clearly evident.

As the dominant reflected signals are from perpendicular velocity fluctuations within the vortex, they have no Doppler shift (other than due to the fall velocity of the vortex) and as a result there is minimal range error so that the structure of the vortex velocity determined from the reflected signal level will yield the correct vortex structure. Any range error induced by the vortex fall velocity will affect all of the measurements in a similar way so that the vortex velocity structure will not be significantly distorted. Any ambient wind will be orthogonal to the vertical beam so that there will be minimal effect on the measurements from the wind. Doppler vortex measurements by Burnham noted that the acoustic vortex sounder using Doppler measurements "is well suited for measuring vortex strength which depends upon the slowly varying velocity field away from the core[7]". In other words, direct measurements of the vortex core characteristics using Doppler techniques are not possible, this restriction means that it is difficult to measure the whole vortex structure using Doppler, this restriction is probably also the case for making Doppler measurements by LIDAR.

3. Measurements of wake vortex characteristics

The use of the vortex reflected amplitude to measure the whole vortex structure in great detail in a perpendicular direction is shown in the following direct vortex measurements. To display the wake measurement results, simultaneous measurement for each of the 8 acoustic transceivers used in the wake measurement array shown in Figure 3 is shown in the same time frame, with an x axis of seconds elapsed since the aircraft passed over the array at a height of around 60m (see Figure 5). The acoustic transceivers are spread out over a distance of 157m orthogonal to the aircraft direction at a distance of 990m from the runway threshold. A vertical red line shows when the aircraft passed over the array as is due to the aircraft noise .

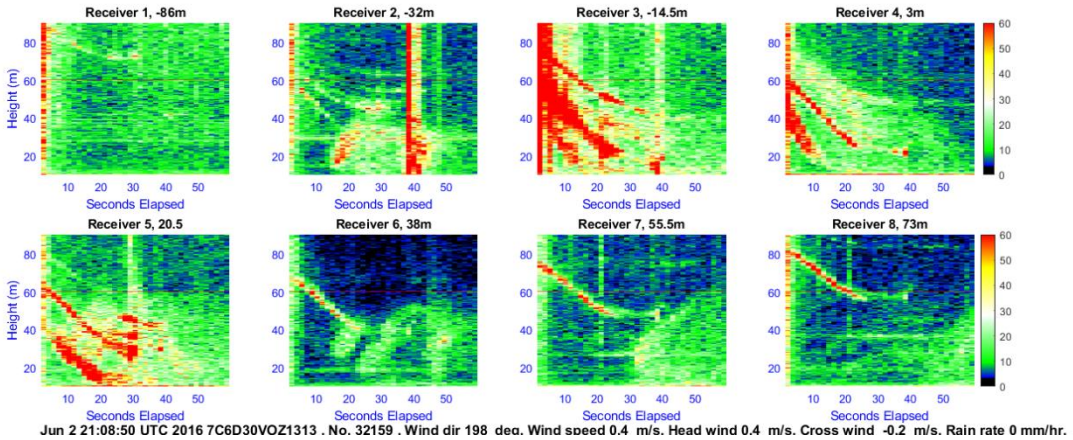

Figure 5. Example wake vortex measurement of a B738 arrival at a height of 60m above the wake array shown in Figure 3. The data updates every 1.57 seconds with a vertical resolution of 0.2m to a height of 90m. In this picture the aircraft was overhead of the array at 0 seconds at a height of about 60m. The time to the right is seconds elapsed since the aircraft was overhead at 0 seconds. Signal level is in volts above the noise level. The detailed structure of the atmosphere at the time of this measurements is shown in Figure 21.

In Figure 5 the port side of the array for this arrival is shown by negative array distances of -86m, -32m, -14.5m from the approach centre line while the starboard side is measured by the receivers at 20.5m, 38m, 55.5m, and 73m. The port vortex is evident in the receiver 3 that is -14.5m to port from the approach centre line. The starboard vortex is visible in receiver 5 at 20.5m. Both vortices fall at around 1.5m/s. The port vortex drifts over receiver 2 at -32m, 38 seconds after the aircraft is overhead in a starboard to port cross-wind of -0.5m/s. The port vortex breaks up after 42 seconds as is shown by the vertical line at 42 seconds in receiver 2 which is due to the noise of the vortex break-up. The starboard vortex measured by receiver 5 at 20.5m to starboard, is stalled and seen by receiver 5 to break up at 30 seconds. The signal level shown in the colour bar is in Volts. As the noise level is around 1 volt, the signal to noise from a wake vortex can exceed 50 times the noise (34dB S/N). If the signal from the vortex is above 34dB it will show as red indicating a high level of wake vortex reflected signal and correspondingly high velocity fluctuations. The signals shown the receivers 6, 7 and 8 at 38m, 55.5m, 73m respectively are secondary responses from the primary starboard vortex at 20.5m and are due to their signals being reflected from the vortex core at 20.5m, this is evident by the increasing altitude of the responses for receivers 6,7 and 8 indicating longer path lengths from the vortex receiver 5 at 20.5m. The signal shown in receiver 4 at 3m is a composite of the port and starboard vortices. Vortices also show as coherent structures with well defined peaks of the vortex core. The complex atmospheric structure shown in Figure 21 is for the same time period as the measurement of Figure 5.

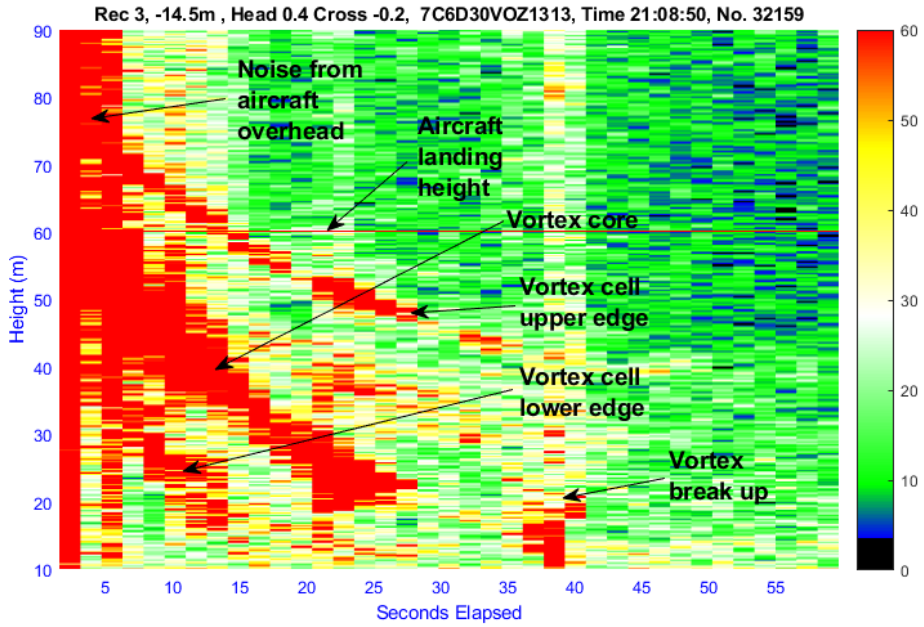

Figure 6. A detailed image of the data for receiver 3 at -14.5m to port from Figure 5. The vertical resolution is 0.2m and the horizontal resolution is 1.57 seconds. The B738 is overhead at time 0 on the left at height of 60m, (left vertical red line). The core vortex falls from the height of the aircraft at 60m at a rate of 1.5m/s. The horizontal red line at 60m shows the approach height of the aircraft over the array. Highlights of the image are shown.

In Figure 6 all signals above 50 (34dB S/N) are show in red. The amplitude reference level is 0 which is the level of the background noise. The core of the vortex can be seen starting at a height just below 60m and continuing on for about 28 seconds after the aircraft has passed ending at a height of around 22m. After 6 seconds the upper edge of the vortex cell is visible at around 70m while the lower edge of the vortex cell is visible at around 35m. The outer edges of the vortex cell can be seen to fall so that at around 13 seconds the upper edge of the cell is around 62m above ground and the lower edge is down to 18m above ground providing a cell diameter at 13 seconds of 44m, indicating that the vortex cell is gradually increasing diameter with age. The vortex drifts out of the receiver 3 aperture after about 35 seconds and breaks up over receiver 2 after 42 seconds has elapsed. The vortex probably demises with an audible noise pulse which can be seen as the vertical line at this time. The core, if present, often demises with an audible crack, probably indicating that the core velocity has exceeded the speed of sound. The noise for wake vortices studied numerically and experimentally[9] and the noise source is closely located to the vortex cores.

Wake vortex structure for B738

Figure 7 below shows the detailed structure of a wake vortex from the B738 measurement detailed in Figure 6 from receiver 3 at 4 seconds after the aircraft has passed overhead. The measurement signal from the vortex is by reflection from the velocity fluctuations of wake vortex before application of the RCS correction of equation 6.

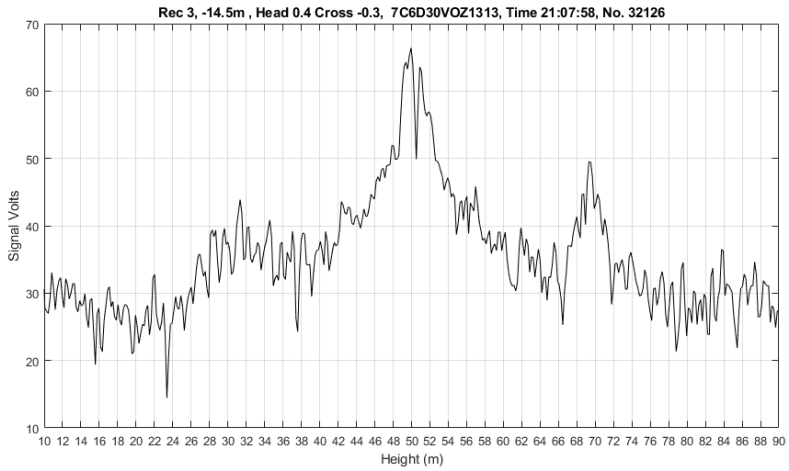

Figure 7. Point measurement of the vertical structure of B738 wake shown in Figure 6 at 4 seconds elapsed time. Receiver 3 is located -14.5m to port from the arrival centre line and sees the port vortex. The vertical resolution is 0.2m. The background noise is around 10dB due to noise associated with the vortex. When no vortices are present the background noise is around 0dB. The return signal is due to reflection from the horizontal velocity fluctuations within the vortex. The diameter of the vortex core is 1m. The diameter of the vortex cell is also shown.

In Figure 7 the core radius of the vortex is 0.5m equal to 0.014 of the wing span. The edges of the vortex are reasonably well defined so that an estimate of the vortex overall diameter can be achieved.

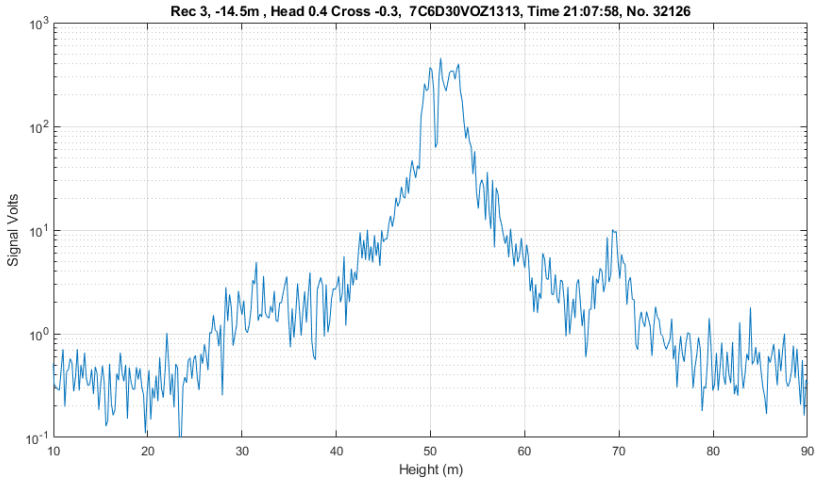

Figure 8. Vortex velocity gradient after the application of equation 6 to correct for the RCS, equation 7 is then applied to this data to obtain the vortex velocity structure, a calibration constant is then applied to obtain the actual velocity structure.

The vortex structure shown in Figure 9 below is integrated in the manner shown in equation (7) using the data of Figure 8. The use of equation 7 assumes that the vortex velocity is zero at the vortex edges and passes through zero in the core, the integration is thus achieved in two parts, one for negative velocity and one for positive velocity components. The integration also assumes that

the peak velocity is located at the points that satisfy the needs for the wake vortex velocity to be zero at the edges, in other words the sign of the integration changes at the point of peak velocity which enables the core to be defined.

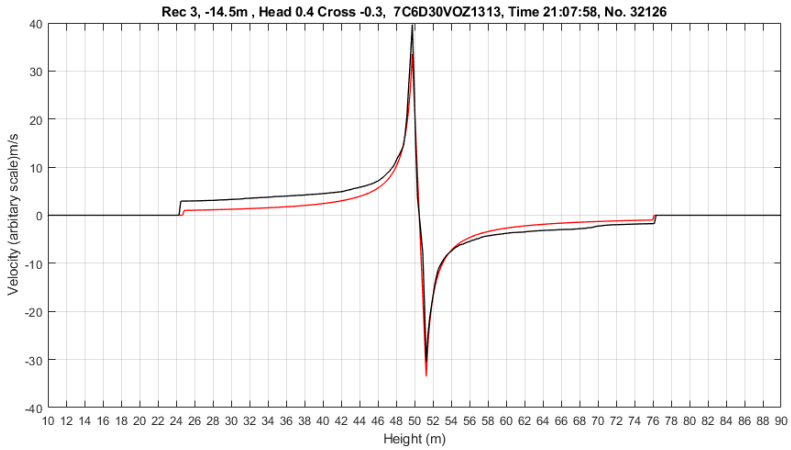

Figure 9 . Estimation of the B738 vortex velocity structure from the measured data of Figure 8. This the same result as shown in Figure 2.

The measured vortex core diameter shown in Figure 7 and Figure 9 is 1m. Using a radius of 0.5m for the modelled vortex and a circulation of 160m^2/s results in a very good fit of the model to the data.

Wake vortex structure for A333

Shown below is an example of a long lasting wake vortex with examples of the evolution of the vortex structure above an inversion layer.

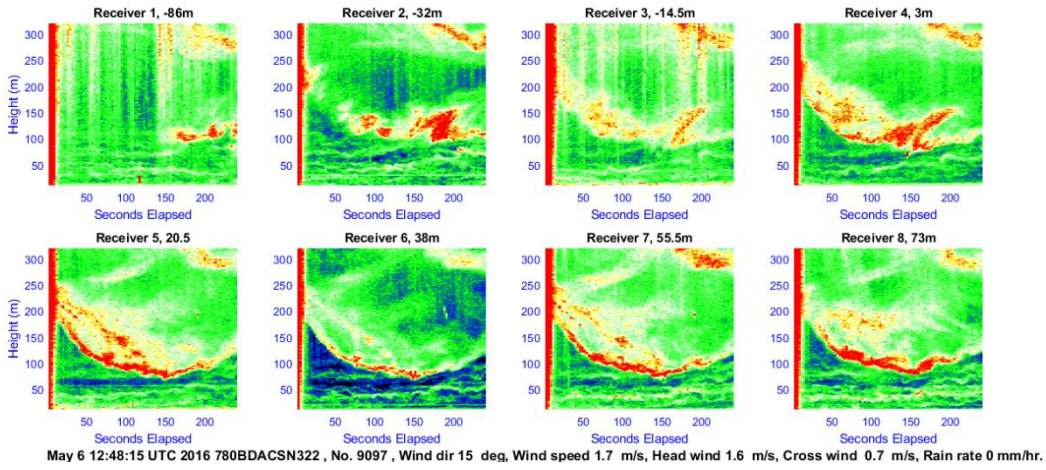

Figure 10 . Signal levels (volts) back scattered from vortices generated by an A333 departure. The departure occurs at a height of around 210m. The data updates every 2.73 seconds with a vertical resolution of 0.7m to a height of 320m. Cross wind is in the direction from receiver 8 towards receiver 1. The detail of the atmosphere structure at the time of this measurements is shown in Figure 22.

In Figure 10 there is an inversion layer present at a height of around 50m which interacts with the generated vortices by an A333 to cause them to rebound. The vortices initially drop at around 2m/s

for 100 seconds and then the descent slows as the vortices start to feel the presence of the inversion layer. The vortices rebound about 150 seconds after the aircraft passes over the array. There are inversion layers above and below the height of the departure so that the turbulence of the atmosphere is very low, this observation being justified by the low level of the acoustic reflected signal commonly seen between inversion layers. The result is that there is very little interaction of the vortex with the atmosphere because the very low turbulence above the inversion layer allows the vortex to be self sustaining and the vortex is very long lived. The detail of the atmosphere for the period of this measurement is shown in Figure 22.

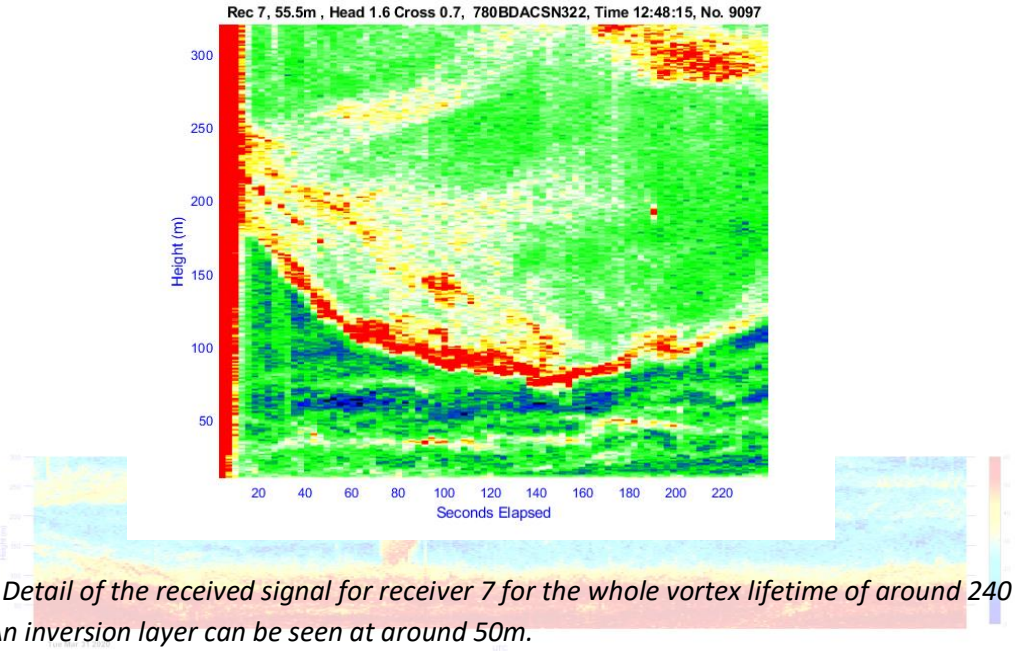

Figure 11. Detail of the received signal for receiver 7 for the whole vortex lifetime of around 240 seconds. An inversion layer can be seen at around 50m.

Figure 11 shows the complete vortex lifetime of the receiver located 55m to Starboard of the approach, the wind speed is 1.6m/s head and a cross wind of 0.7m/s from the port side.

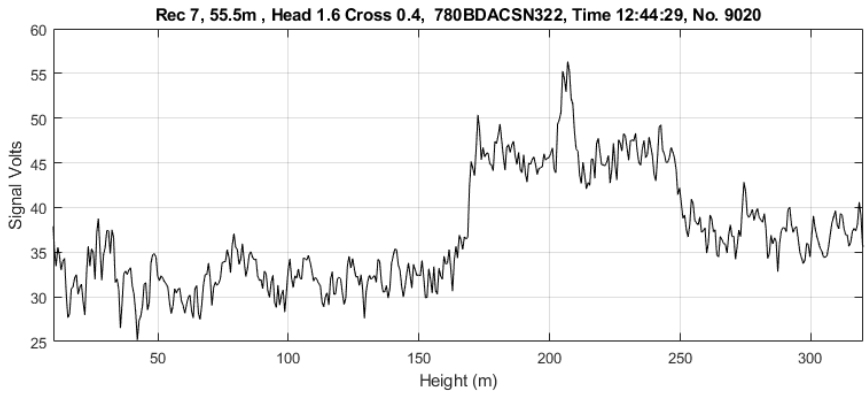

Figure 12. An A333 departure vortex measurement shown in Figure 11 on May 6 2016 showing the vortex at 22 seconds after the aircraft is overhead. The radius of the vortex core is 2m and the diameter of the vortex cell is 95m . The strong vortex associated with the core is very evident.

In Figure 12 the overall vortex structure is very clear and the edges of the vortex are very well defined enabling a accurate estimate of the vortex diameter to be obtained. There is also a very clear and strong vortex core.

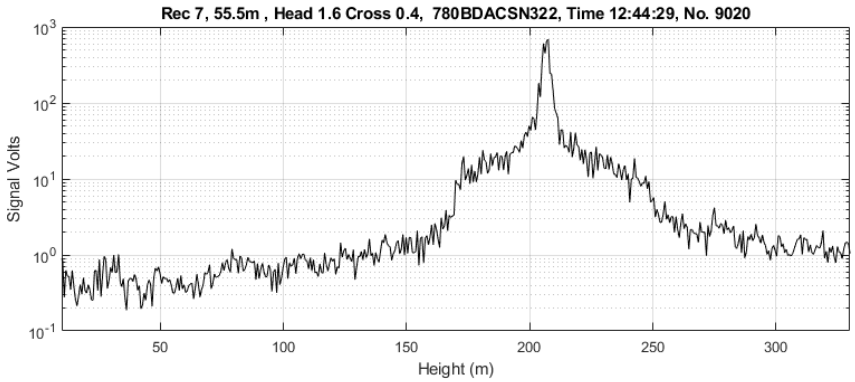

Figure 13. An A333 departure vortex after application of the RCS correction to the data of Figure 12.

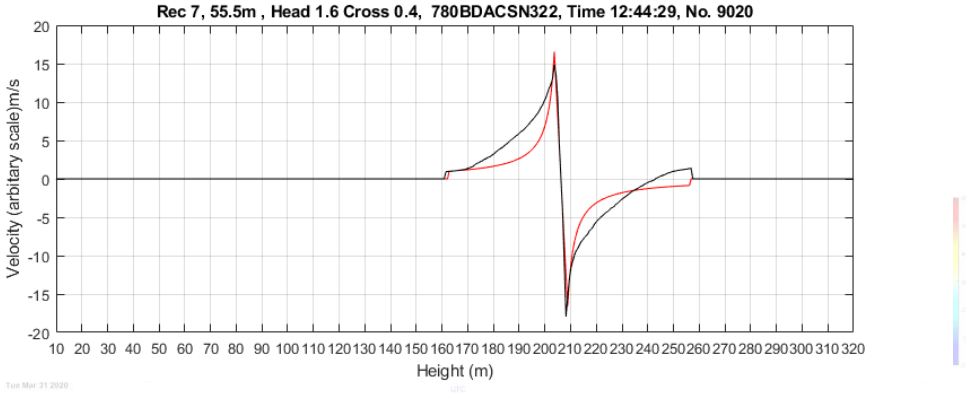

Figure 14. A333 departure wake vortex velocity integrated from Figure 13 above 18 seconds after the aircraft is overhead. Also shown in red is a modelled vortex using a circulation of 297m^2/s and a core radius of 2m.

In Figure 14 a circulation 297m^2/s and assumed core radius of 2m are used to obtain the modelled vortex velocity shown in red.

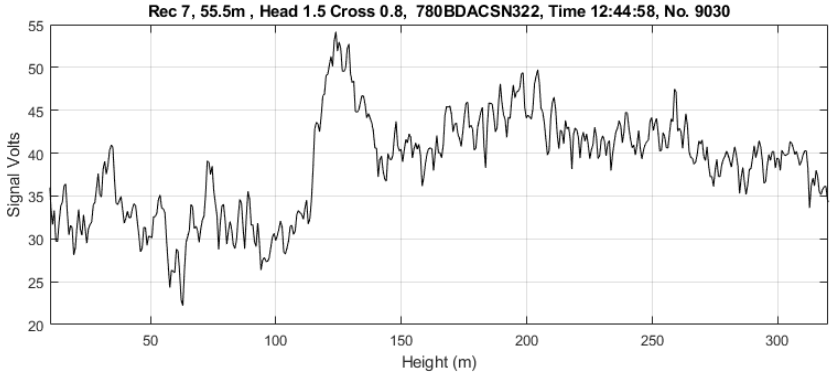

Figure 15. An A333 departure vortex measurement shown in Figure 11 on May 6 2016 showing the vortex at 47 seconds after the aircraft is overhead. The diameter of the vortex cell is 160m .

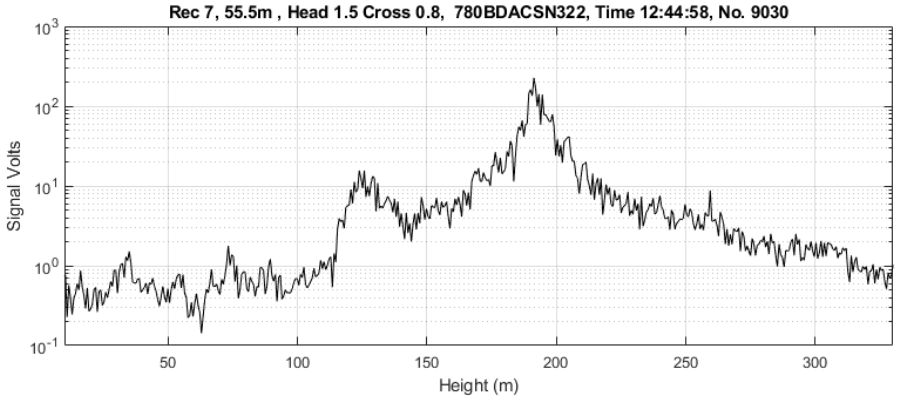

Figure 16. An A333 departure vortex after application of the RCS correction to the data of Figure 15.

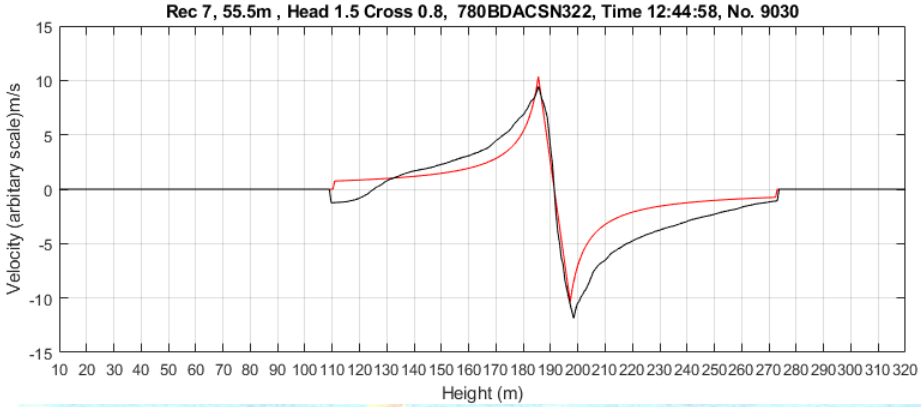

Figure 17. A333 departure wake vortex velocity integrated from Figure 16 above 47 seconds after the aircraft is overhead. Also shown in red is a modelled vortex using a circulation of 380m²/s and a core radius of 7m.

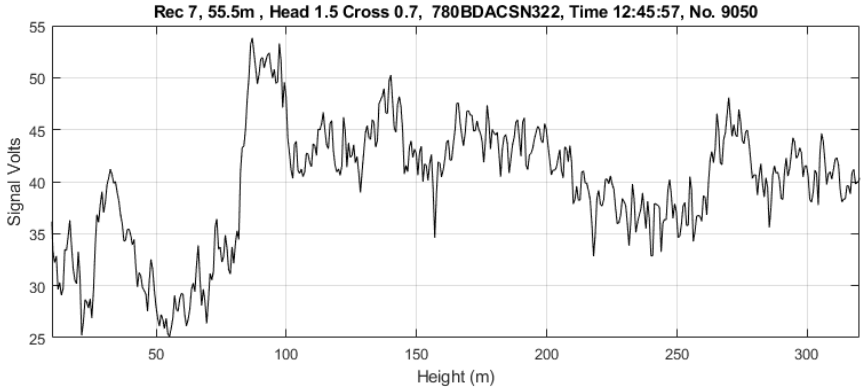

Figure 18. An A333 departure vortex measurement shown in Figure 11 on May 6 2016 showing the vortex at 106 seconds after the aircraft is overhead. The diameter of the vortex cell is 130m .

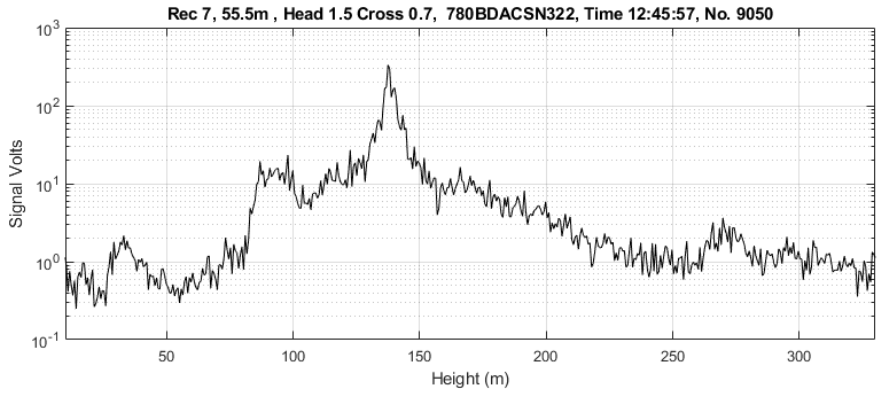

Figure 19. An A333 departure vortex after application of the RCS correction to the data of Figure 18

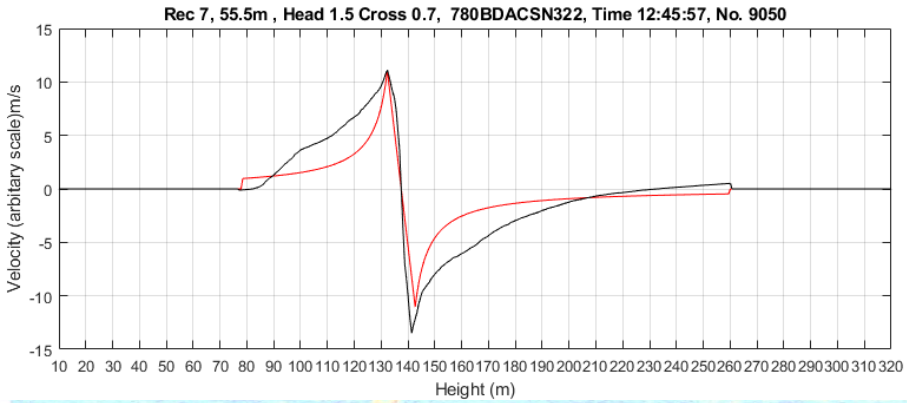

Figure 20. A333 departure wake vortex velocity integrated from Figure 19 above 106 seconds after the aircraft is overhead. Also shown in red is a modelled vortex using a circulation of 360m²/s and a core radius of 5m.

It is evident from the vortex measurements above that as the vortex evolves above an inversion layer its core radius increases and the circulation also increases. The vortex eventually demises at around 240 seconds. The strong circulation and a larger core could be sufficient to cause an upset if encountered by a following aircraft. This may be the first direct evidence of the level of hazard of a long lasting vortex can represent.

4. The effects of atmospheric inversions on vortex lifetime

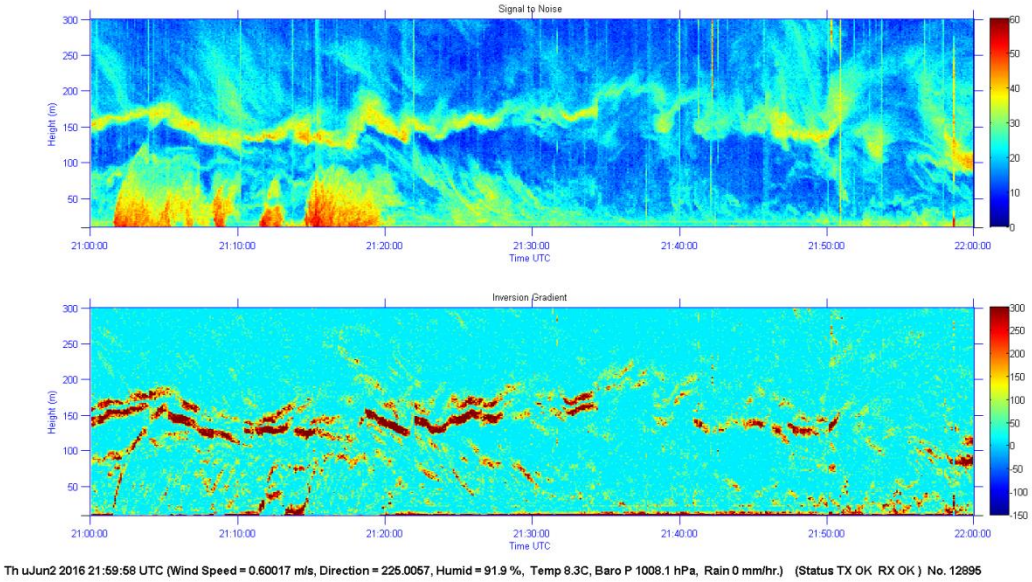

Figure 21. Structure of the atmosphere between 21:00 UTC and 22:00 UTC on Jun 2 2016. During the period shown in this figure the results shown in Figures 5 to 9 were obtained from. The wake from the arriving B738 can be seen just after 21:00. Three other aircraft wakes can be seen at 21:08, 21:12 and 21:15. The wakes are stalled in the very light Easterly wind. The gradient of the atmosphere is also shown so that the delineation and strength of the inversion layers can be clearly seen.

In Figure 21 the reflected signals from the atmosphere are from small scale temperature induced turbulence with the result that changes in atmospheric temperature, such as where inversion layers are present, enables the inversion layers to be clearly seen. Wakes from arriving aircraft are also shown between 21:00 UTC and 21:20 UTC, these reflected signals are from velocity fluctuations directly related to the wake vortices. There is some turbulence below the arrival height of the aircraft at 60m resulting in longer wake lifetimes as the wakes drift over the vertical structure measurement point that is 98m to the starboard of the approach centre line.

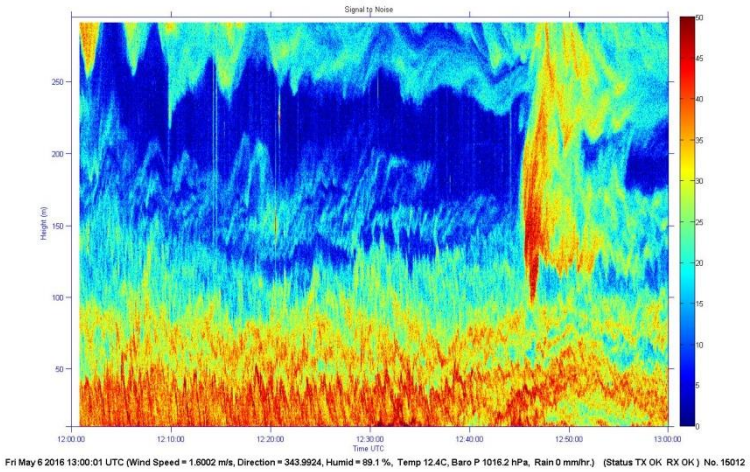

Figure 22. Detail of an elevated inversion on 6 May 2016 between 12:00 UTC and 13:00 UTC. A ground based inversion at 50m is also evident. The A333 departure shown in Figures 10 to 20 is also visible between the inversion layers after 12:45 as the wake vortex drifts to starboard.

Figure 23 shows how the structure of that atmosphere changes over 24 hours. In unstable atmospheres, the wake vortices are short lived because of the associated strong turbulence. When inversion layers are present the wake vortices are longer lived when the turbulence is reduced, particularly above the inversion layers.

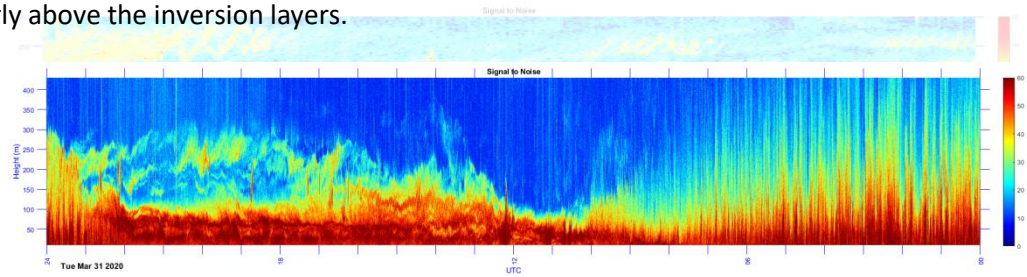

Figure 23. Structure of the atmosphere for 24 hours for Tue 31 March 2020 to a height of 420m. The local daytime is from 00:00 UTC till 09:00 UTC on 30 March and from 22:00UTC till 23:59UTC on 31 March when the atmosphere is unstable. During the night time between 09:00UTC and 22:00UTC the wind direction changes to SW to NW at a speed of around 2 to 6 knots and the inversion layers form.

5. Conclusions

By assuming than the vortices can be modelled by A Rankine structure, the measured wake vortices show reasonable agreement with this model. The use of a chirp SODAR provides the necessary system gain to allow measurements to enable the estimation of the prevailing tangential velocity profiles within a wake vortex with high resolution. Some example vortex measurements and calculations show the detailed structure of these velocity profiles for the first time.

These measurements serve to underline the already recognised importance of atmospheric turbulence in determining wake lifetime, particularly in relation to inversion layers. In the absence of atmospheric turbulence such as above inversion layers, there is very little turbulence to hasten the demise of the vortices so that they are long lived.

The ability to measure vortex velocity profiles in real time will allow rapid assessment of their state and a simplified estimate of their life-times. The increased signal processing gain and greatly improved resolution of a chirp SODAR allows the benefits outlined above to be achieved.

The scaling of the wake vortices was approximately scaled to the calculated circulation for a B738 and A330. Higher turbulence atmospheres appear to have better coupling to the vortices which results in short vortex lifetimes while very low turbulence atmospheres have poor coupling to the vortices which results longer vortex lifetimes associated with an increase in vortex core radii. These longer lived vortices with their larger core radii and consequently greater circulation could be the principal cause of sever wake encounters.

The use of this wake vortex measurement technique will provide a new understanding of the nature of wake vortices to be obtained at far higher resolution than other systems provide. This will enable the characteristics of long lived wake vortices to be investigated to promote the development of appropriate aircraft spacing rules when inversion layers are detected.

References.

1/ James N. Hallock, Frank Holzäpfel, "A Review of Recent Wake Vortex Research for Increasing Airport Capacity", Progress in Aerospace Sciences, Vol. 98, April 2018, pp 27-36. https://core.ac.uk/reader/154792303

2/ S.M. Mackey & D.C. Burnham, "Use of a Commercial Wind SODAR for Measuring Wake Vortices", 12th AIAA/CEAS Aero-acoustics Conference, 8-10 May 2006, Cambridge MA, pp 1-5.

3/ S. Bradley, "Atmospheric Acoustic Remote Sensing", CRC Press, ISBN 978-0-8493-3588-4, 2008, pp40.

4/ J. Hallock and W. R. Eberle, 1977: Aircraft wake vortices: A state-of-the-art review of the U.S. R&D Program. Federal Aviation Administration Rep. FAA-RD-77-23, 326 pp. [Available from National Technical Information Service, Sills Bldg., 5285 Port Royal Rd., Springfield, VA 22161.] (Hallock and Eberle 1977).

5/ F.Holzapfel, T. Hofbauer, T. Gerz, & U. Schuman, "Aircraft Wake Vortex Evolution and Decay In Idealized and Real Environments: Methodologies, Benefits and Limitations". http://www.pa.op.dlr.de/wirbelschleppe/publ/EUROMECH412.pdf

6/ F.Holzapfel, "Aircraft Wake Vortex Evolution and Prediction", Mechanical Engineering, Technical University of Munich, 12 October 2005.

7/ D.C Burnham & T.E. Sullivan, "Measurement of Wake Vortex Strength by Means of Acoustic Back Scattering", Journal of Aircraft, Vol 10, No 11, November 1976, pp 889-894. https://arc.aiaa.org/doi/10.2514/3.44559

8/ Nash'at N. Ahmad, Fred H. Proctor, Fanny M. Limon Duparcmeur, Don Jacob, " Review of Idealized Aircraft Wake Vortex Models", American Institute of Aeronautics and Astronautics, 10 Jan 2014. DOI: 10.2514/6.2014-0927, 52nd Aerospace Sciences Meeting, National Harbor, Maryland, USA.

9/ P. Böhning, U. Michel and R. Baumann, ’ Acoustic Properties of Aircraft Wake Vortices’, DLR, 2008, oai:elib.dlr.de:55784, https://elib.dlr.de/55784/1/FB4.pdf

10/ https://en.wikipedia.org/wiki/Rankine_vortex

11/ S. Bradley, "Atmospheric Acoustic remote Sensing", CRC Press, 2008, ISBN 13:978-0-8493-3588-4.